RESEARCH ARTICLE

Aging Cell

WILEY

Deficiency for scavenger receptors Stabilin-1 and Stabilin-2 leads to age-dependent renal and hepatic depositions of fasciclin domain proteins TGFBI and Periostin in mice

Thomas Leibing[1,2] ⓘ | Anna Riedel[1,2] | Yannick Xi[1,2] | Monica Adrian[1,2] |
Jessica Krzistetzko[1,2] | Christof Kirkamm[1,2] | Christof Dormann[1,2] | Kai Schledzewski[1] |
Sergij Goerdt[1,3] | Cyrill Géraud[1,2,3]

[1]Department of Dermatology,
Venereology and Allergology, University
Medical Center and Medical Faculty
Mannheim, Heidelberg University,
Mannheim, Germany

[2]Section of Clinical and Molecular
Dermatology, University Medical
Center and Medical Faculty Mannheim,
Heidelberg University, Mannheim,
Germany

[3]European Center for Angioscience
(ECAS), Medical Faculty Mannheim,
Heidelberg University, Mannheim,
Germany

Correspondence
Thomas Leibing and Cyrill Géraud,
Department of Dermatology, Venereology
and Allergology, University Medical
Center and Medical Faculty Mannheim,
Heidelberg University, Theodor-Kutzer-
Ufer 1-3, 68167 Mannheim, Germany.
Email: thomas.leibing@umm.de and
cyrill.geraud@umm.de

Funding information
Deutsche Forschungsgemeinschaft,
Grant/Award Number: INST 35/1503-1
FUGG, 259332240, 394046768, 5454871,
5486332 and INST 35/1314-1 FUGG;
Ministerium für Wissenschaft, Forschung
und Kunst Baden-Württemberg, Grant/
Award Number: INST 35/1503-1 FUGG

Abstract

Stabilin-1 (Stab1) and Stabilin-2 (Stab2) are two major scavenger receptors of liver si-
nusoidal endothelial cells that mediate removal of diverse molecules from the plasma.
Double-knockout mice (Stab-DKO) develop impaired kidney function and a decreased
lifespan, while single Stabilin deficiency or therapeutic inhibition ameliorates athero-
sclerosis and Stab1-inhibition is subject of clinical trials in immuno-oncology. Although
POSTN and TFGBI have recently been described as novel Stabilin ligands, the dynam-
ics and functional implications of these ligands have not been comprehensively stud-
ied. Immunofluorescence, Western Blotting and Simple Western™ as well as in situ
hybridization (RNAScope™) and qRT-PCR were used to analyze transcription levels
and tissue distribution of POSTN and TGFBI in Stab-KO mice. Stab-POSTN-Triple de-
ficient mice were generated to assess kidney and liver fibrosis and function in young
and aged mice. TGFBI and POSTN protein accumulated in liver tissue in Stab-DKO
mice and age-dependent in glomeruli of Stabilin-deficient mice despite unchanged
transcriptional levels. Stab-POSTN-Triple KO mice showed glomerulofibrosis and a
reduced lifespan comparable to Stab-DKO mice. However, alterations of the glomeru-
lar diameter and vascular density were partially normalized in Stab-POSTN-Triple KO.
TGFBI and POSTN are Stabilin-ligands that are deposited in an age-dependent man-
ner in the kidneys and liver due to insufficient scavenging in the liver. Functionally,
POSTN might partially contribute to the observed renal phenotype in Stab-DKO mice.
This study provides details on downstream effects how Stabilin dysfunction affects
organ function on a molecular and functional level.

KEYWORDS
aging, fasciclin, lifespan, mouse, POSTN, scavenger receptors, TGFBI

1 | INTRODUCTION

During tissue turnover and regeneration, contents of the extracellular matrix, such as collagens and connective tissue polysaccharides are released into the plasma to a certain extent. Those molecules are cleared and degraded by scavenger receptors expressed by liver sinusoidal endothelial cells (LSECs) (Bhandari et al., 2021). Stabilin-1 (Stab1) and Stabilin-2 (Stab2) are the two members of the class H Scavenger Receptors expressed by LSECs, which contain EGF-like, laminin EGF-like (https://www.uniprot.org/uniprotkb/Q9NY15/entry) and fasciclin domains (PrabhuDas et al., 2017). They each have distinct, but also common ligands, based on the functionality of several domains (Harris & Cabral, 2019; Patten & Shetty, 2019). For example, hyaluronic acid is only bound by Stab2, while Stab1 is unable to ibind hyaluronic acid, likely due to differences in link domain function (Hansen et al., 2005; Politz et al., 2002). Previously, we showed that Stab1/Stab2-double-knockout mice (Stab-DKO) present an impaired kidney function and a decreased lifespan likely due to their impaired scavenging function through LSECs (Schledzewski et al., 2011). Only recently, we were able to show that single Stabilin inhibition reduces atherosclerosis development (Manta et al., 2022), furthermore, anti-Stab1 antibodies are in initial clinical trials as an immunomodulatory cancer treatment (Virtakoivu et al., 2021). Mechanistically, we were able to show that extracellular matrix proteins Transforming growth factor, beta-induced, 68 kDa (TGFBI) and Periostin (POSTN) are ligands of Stab1 and Stab2, likely due to fasciclin domain interactions. Their plasma concentration is strongly increased in Stab-DKO mice (Manta et al., 2022). Interestingly, Stab1 and Stab2 as well as POSTN and TGFBI are the only four fasciclin-domain containing proteins in mammals (Seifert, 2018). POSTN is implicated as a causative agent in a plethora of fibrotic diseases: Knockout of POSTN in mice protects from CCl_4-induced liver injury (Kumar et al., 2018) as well as unilateral ischemia–reperfusion injury induced kidney fibrosis (An et al., 2019). Additionally, it is implicated as a biomarker for disease severity in kidney disease (Guerrot et al., 2012; Satirapoj et al., 2014, 2015; Wantanasiri et al., 2015). Interestingly, aged POSTN-KO C57BL/6J mice show ameliorated kidney fibrosis compared to WT C57BL/6J mice after 24 months, while overall survival is unaffected (An et al., 2021). TGFBI is described as a modulator of cell-collagen interaction and thus seems likely to contribute to fibrous disease pathways (Billings et al., 2002; Hanssen et al., 2003). As TGFBI and POSTN constitute paralogs it seems probable that both proteins contribute in certain diseases (Schwanekamp et al., 2016). Stab1 and Stab2 single inhibition mediates beneficial effects in atherosclerosis development (Manta et al., 2022), anti-Stab1 inhibition is in clinical trials in immune-oncology (Virtakoivu et al., 2021). We here assess the possible side effects of single and double Stabilin deficiency or inhibition on the scavenging of POSTN and TGFBI from the circulation and their tissue distribution.

2 | METHODS

2.1 | Animals

All animal experiments were performed in accordance with local regulatory institutions (Regierungspräsidium Karlsruhe). All mice were bred on a C57BL/6J background in the animal facilities of the Centre for medical research, Medical Faculty Mannheim. Stab1-KO (B6.129S2-Stab1^tm1.1Cger; Schledzewski et al., 2011) and Stab2-KO (B6.129S2-Stab2^tm1.1Cger; Schledzewski et al., 2011) mice were interbred to generate transgenic mice with Stabilin-double deficiency (Stab-DKO). Stab-DKO mice were bred to POSTN-KO mice (B6;129-Postn^tm1Jmol/J; Oka et al., 2007) to generate Stab-POSTN-Triple deficient mice (Stab-POSTN-TrKO). Male and female mice were pooled for analysis except in Figure S1. Genotyping was performed as described earlier (Oka et al., 2007; Schledzewski et al., 2011).

2.2 | Immunofluorescence

PFA-fixed and paraffinized liver and kidney tissue was sectioned at 4 μm. Deparaffinization, rehydration, and antigen retrieval were performed as previously described (Leibing et al., 2018). Primary antibodies (Table S1) were incubated overnight and secondary antibodies (DIANOVA) for 1 h.

2.3 | Quantification of staining intensities in IF-stainings of glomeruli

Microscopy images of kidney samples were prepared for analysis by using "Rolling Ball" and "Extended Depth of Focus" from the NIS Elements (Version 5) software. Glomeruli were defined as ROIs by Freehand selection in a merged channel view. After importing all ROIs of an image into the ROI manager, quantification was performed on single channel images. Thresholding was performed using the "Otsu dark" Auto Threshold filter. Data were collected for area of the ROI and percentage of area with positive staining signal and later used to calculate total positive staining area of the glomeruli. The Macro used for DAPI/EMCN/TGFBI/Postn and DAPI/EMCN/SPARC co-staining is attached in the appendix (Table S1). Signal intensities were quantified in liver area using thresholding in ImageJ 1.53 (Schneider et al., 2012).

2.4 | Simple Western

Simple Western was performed according to manufacturer's protocols (Harris, 2015; Lück et al., 2021). Primary antibodies are found in Table S1.

2.5 | Western blotting

Kidney and liver tissue were homogenized in RIPA and were analyzed by SDS-Page and Immuno-blotting on PVDF membranes as by the manufacturer protocol (Trans-Blot Turbo Transfer System, Bio-Rad). Incubation with primary antibodies (Table S1) was performed at 4°C overnight at a 1:1000 dilution in 5% nonfat dry milk (Bio-Rad No. 1706404). Incubation of HRP conjugated secondary antibody (different species, Dianova) was performed for 1h at room temperature. Chemiluminescence (Millipore WBLUF0500) intensity detection was performed with the Azure® c400 imaging system (Azure® Biosystems) and quantified using ImageJ 1.53 (Schneider et al., 2012).

2.6 | RNA in situ hybridization

PFA-fixed and paraffinized liver and kidney tissue was sectioned at 4μm. A modified non-isotopic in situ hybridization protocol was carried out using the RNAscope 2.5 HD Red kit (Advanced Cell Diagnostics) following the manufacturer's recommended protocol with specific probes against the positive control mouse Ppib (Cyclophilin B) gene and mouse POSTN or TGFBI (Table S1). Sections were ultimately stained with DAB and counterstained with hematoxylin.

2.7 | Urinalysis

Animals of the same genotype were arranged in groups of 6–8 and followed for an observation period of up to 2years. Mice were housed in metabolic cages for 24h to collect urine samples. Urine was analyzed for Protein and Albumin (Cobas c 311 Analyzer; Roche Diagnostics).

2.8 | Statistics

Statistical analyses were performed with JMP® 16 and SAS® 9.4M7 (SAS Institute Inc.). For comparisons between two groups, t test was used when the normality assumption was met using the Shapiro–Wilk test. For group comparisons of three groups, the one-way ANOVA was used when the normality assumption was met using the Shapiro–Wilk test. We used the Brown-Forsythe test to check for equal variances. In case of unequal variances, the Welch ANOVA was used. Tukey–Kramer HSD was used as a post hoc tests for groups of three. For group comparisons of four or more groups, the one-way ANOVA was used when the normality assumption was met using the Shapiro–Wilk test. We used the Brown-Forsythe test to check for equal variances. In case of unequal variances, the Welch ANOVA was used. For post hoc analyses after significant ANOVA p-values, Dunnett's test was used. If the normality assumption was not met, we used a Kruskal–Wallis test followed by Steel's multiple

comparison test. Reference groups for Dunnett's test or Steel with control were WT mice. Differences between data sets with $p < 0.05$ in t test, ANOVA, Kruskal–Wallis test and post hoc tests were considered statistically significant. For comparison of old and young animals, Standard Least Squares with emphasis on Effect leverage was used. Effects of age, genotype and a full factorial analysis of Age*Genotype was performed. Test slices were used to compare different ages in a single genotype.

2.9 | RT-PCR

Reverse transcription (RT) into complementary DNA (cDNA) was conducted using Maxima Reverse Transcriptase (EP0752, Thermo Fisher Scientific) and Oligo(dT)18 primer (SO131, Thermo Fisher Scientific). Quantitative PCR (qPCR) was performed using innuMIX qPCR SyGreen Sensitive (845-AS-1310200, Analytik Jena) on a qTOWER 3G touch thermal cycler (Analytik Jena). Primers for RT-qPCR were designed using NCBIs PrimerBLAST (https://www.ncbi.nlm.nih.gov/tools/primer-blast/). If possible, primer pairs (Table S1) were designed to span an exon-exon junction, thus being mRNA-specific. If this was not possible they needed to be separated by at least one intron. Primers were validated using no template controls, no RT controls, agarose gel electrophoresis and melt curve analysis. Amplification data were analyzed using qPCRsoft 4.0.8.0 (Analytik Jena). Normalized expression values were calculated using the Pfaffl method considering amplification efficiency values determined by standard curves.

3 | RESULTS

3.1 | Stabilin ligand POSTN is more abundant in aged, enlarged Stab-DKO glomeruli and liver tissue compared to WT

Immunofluorescence revealed an increased abundance of Stabilin-ligand POSTN in glomeruli from aged (12months old) Stab-DKO mice compared to aged WT mice (Figure 1a). Quantification revealed Stab1-KO and Stab2-KO glomeruli did not show significant alterations in POSTN abundance compared to WT (Figure 1b). Stab-DKO glomeruli were significantly larger than WT glomeruli, Stab1-KO and Stab2-KO glomeruli diameter did not reach significance (Figure 1c). Furthermore, perisinusoidal POSTN staining in Stab-DKO livers was observed, which was absent in WT mice (Figure 1d).

3.2 | POSTN expression is unaltered in Stab-DKO tissues, indicating deposition from plasma

To explore the mechanism of increased POSTN abundance, we performed RNA-ISH for POSTN in glomeruli and liver tissue of aged Stab-DKO mice in comparison to WT mice. Furthermore, we
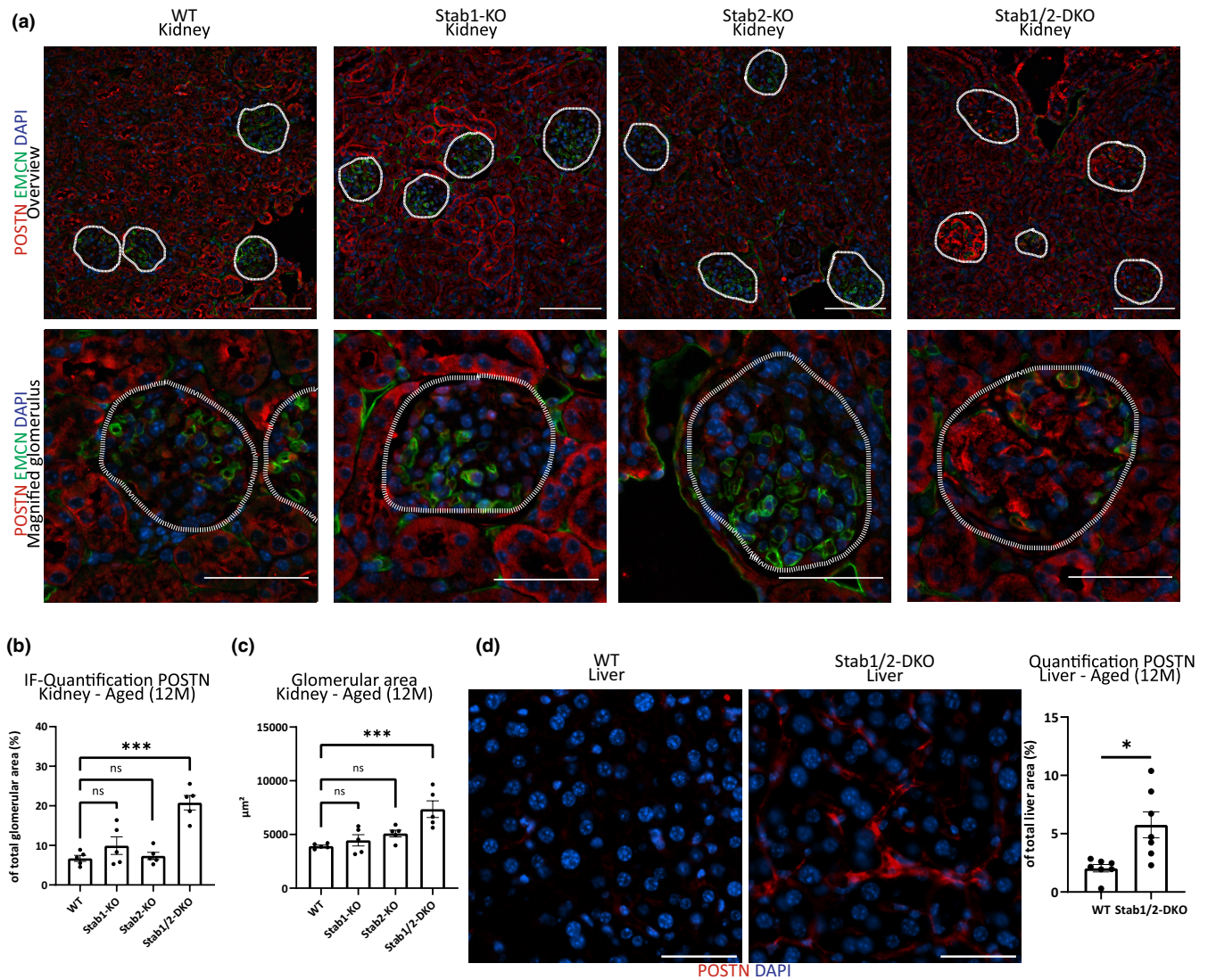
FIGURE 1 POSTN in kidneys and liver from Stabilin-deficient animals. (a) Representative photomicrographs of kidney tissue (upper lane: Overview, Scale bar = 100 μm; lower lane: Magnified glomeruli, Scale bar = 50 μm.) co-stained with DAPI (blue), EMCN (green), and POSTN (red). Dashed white line marks glomeruli. (b) Quantification of average POSTN-positive area in glomeruli (in % of total glomerular area). (c) Quantification of average glomerular diameter (in μm²). (d) Representative photomicrographs of liver tissue co-stained with DAPI (blue) and POSTN (red). Quantification of average POSTN-positive area of total photomicrograph area is shown on the right (in % of total photomicrograph area). $N \geq 5$ for all experiments. Ns = not significant, $*p < 0.05$; $**p < 0.01$; $***p < 0.001$.

performed qRT-PCR of kidney lysate and liver lysate. Here, no difference in the RNA staining pattern and expression levels in kidney and liver (Figure 2) were found, indicating no increased transcription and thereby no increased production of POSTN in both organs in Stab-DKO mice, suggesting a deposition due to increased plasma levels.

3.3 | Genetic ablation of POSTN does not rescue shortened lifespan, glomerulofibrosis and albuminuria observed in Stab-DKO mice

To assess whether POSTN depositions in Stab-DKO glomeruli and liver tissue might be causative for the observed glomerulofibrotic nephropathy and reduced lifespan in Stab-DKO mice, we crossed POSTN-KO mice with Stab-DKO mice. Stab-POSTN-TrKO mice were viable but showed a similarly shortened lifespan comparable to Stabilin-DKO mice (Figure 3a). Age-related mortality was comparable between male and female mice (Figure S1). Urinalysis of aged WT, Stab-DKO, and Stab-POSTN-TrKO mice revealed comparable proteinuria and albuminuria in Stab-DKO and Stab-POSTN-TrKO which was absent in WT mice (Figure 3b). POSTN staining was not observed in Stab-POSTN-TrKO glomeruli and livers serving as negative control supporting the specificity of our previous findings (Figure S2a).

To further explore possible phenotypic alterations in Stab-POSTN-Triple deficient mice, PAS staining of kidneys from aged WT, Stab-DKO, and Stab-POSTN-TrKO were performed. No obvious differences between PAS-positivity in glomeruli Stab-DKO
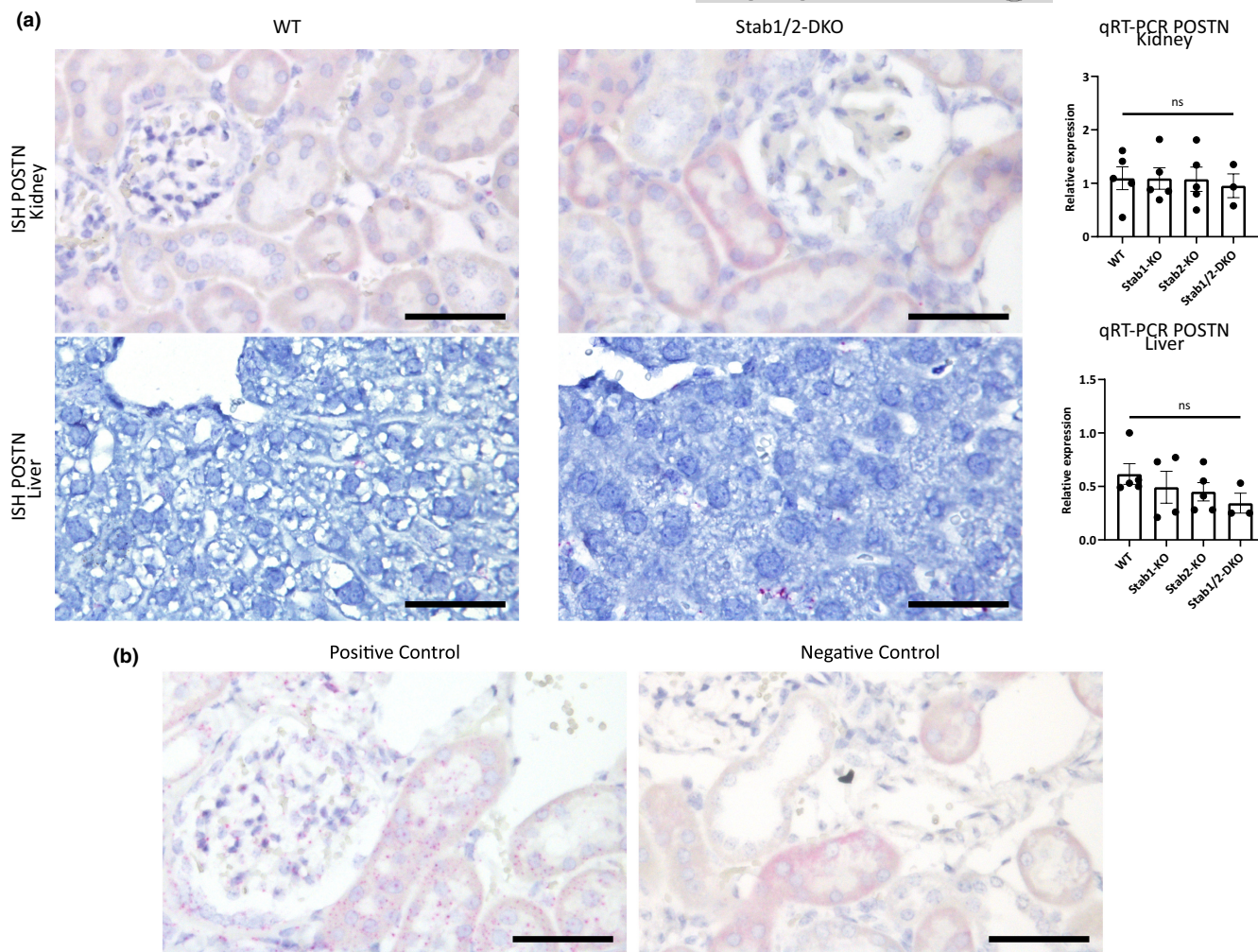
FIGURE 2 Local POSTN transcription is unaltered despite increased protein levels. (a)Left panel: In situ hybridization and Right graph: rt-PCR of Kidney (upper panel) and Liver (lower panel) in WT and Stab-DKO animals for POSTN. (b) Positive Control (Dapß) and negative Ctrl (PPIB). Scale bar = 50 μm. $N \geq 3$ for all experiments. Ns = not significant, $*p < 0.05$; $**p < 0.01$; $***p < 0.001$.

and Stab-POSTN-TrKO was observed, WT glomeruli did not display large amounts of PAS-positive material. Stab-POSTN-TrKO appeared slightly smaller than Stab-DKO glomeruli (Figure 3c). To conform our findings, we quantified the glomerular area, vascular density (using EMCN as a surrogate) and podocyte coverage (using SPARC as a surrogate) in immunofluorescence stainings for DAPI, EMCN and SPARC (Figure 3d) which revealed enlarged glomeruli with a reduced vascularized area in Stab-DKO and Stab-POSTN-TrKO compared to WT (Figure 3e). Slight differences were found between Stab-DKO and Stab-POSTN-TrKO, as Stab-POSTN-TrKO showed a smaller glomerular are and a higher vascularized glomerular area compared to Stab-DKO (Figure 3e). Interestingly, Podocyte marker SPARC showed a similar staining pattern and abundance relative to glomerular area in all genotypes, indicating a lack of podocyte involvement in the type of glomerulofibrosis and reduced vascularization observed in Stab-DKO and Stab-POSTN-TrKO mice (Figure 3e,f).

Liver fibrosis levels were scored using Sirius-red quantification, which did not show significant differences in Sirius-red positive areas between Stab-DKO and Stab-POSTN-TrKO mice but were elevated compared to WT in both knockout mice lines (Figure S2b).

3.4 | Stabilin ligand TGFBI is highly abundant in diseased glomeruli and livers from Stabilin-deficient animals

Since genetic deletion of POSTN did not rescue the phenotype of double-Stabilin deficiency, we assessed abundance of another newly identified Stabilin-ligand containing fasciclin domains, TGFBI, in glomeruli of Stabilin-deficient animals. Interestingly, TGFBI showed a similar pattern staining compared with POSTN in immunofluorescent stainings and colocalized with POSTN both in kidneys (Figure 4a, Figure S3a,b) and liver (Figure S3c,d) in Stab-DKO. POSTN colocalized partially with Collagen 1 in glomeruli (Figure S3b) and in midzonal liver lobulus areas (Figure S3d) as indicated by pericentral LSEC marker EMCN and immunofluorescent co-staining, although a much better co-localization of POSTN and TGFBI was observed.
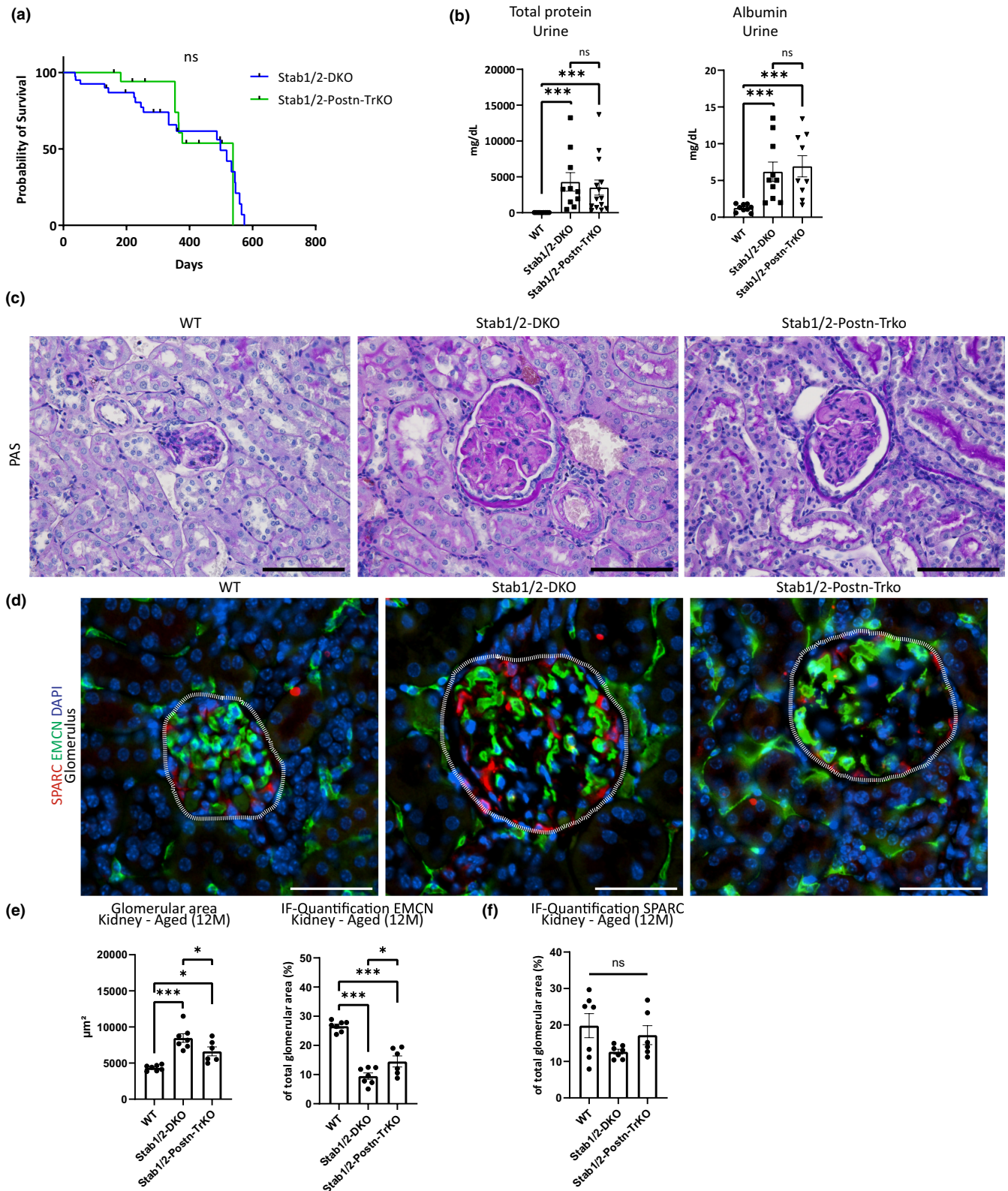
FIGURE 3 Ablation of POSTN does not influence kidney phenotype in Stab-DKO mice. (a) Survival curve of Stab-DKO mice ($n = 40$) and Stab-POSTN-Triple deficient mice ($n = 18$). (b) Total protein and Albumin levels in different mice strains were assessed (c) Representative photomicrographs of PAS-stained kidney tissue from different mice strains. (d) Representative photomicrographs of kidney tissue co-stained with DAPI (blue), EMCN (green), and SPARC (red). Dashed white line marks glomeruli. (e) Quantification of glomerular diameter and EMCN-positivity in total glomerular area, (f) Quantification of SPARC-positivity in total glomerular area. Scale bar $= 50\,\mu m$. $n \geq 5$ for all experiments. ns $=$ not significant, $^*p < 0.05$; $^{**}p < 0.01$; $^{***}p < 0.001$.
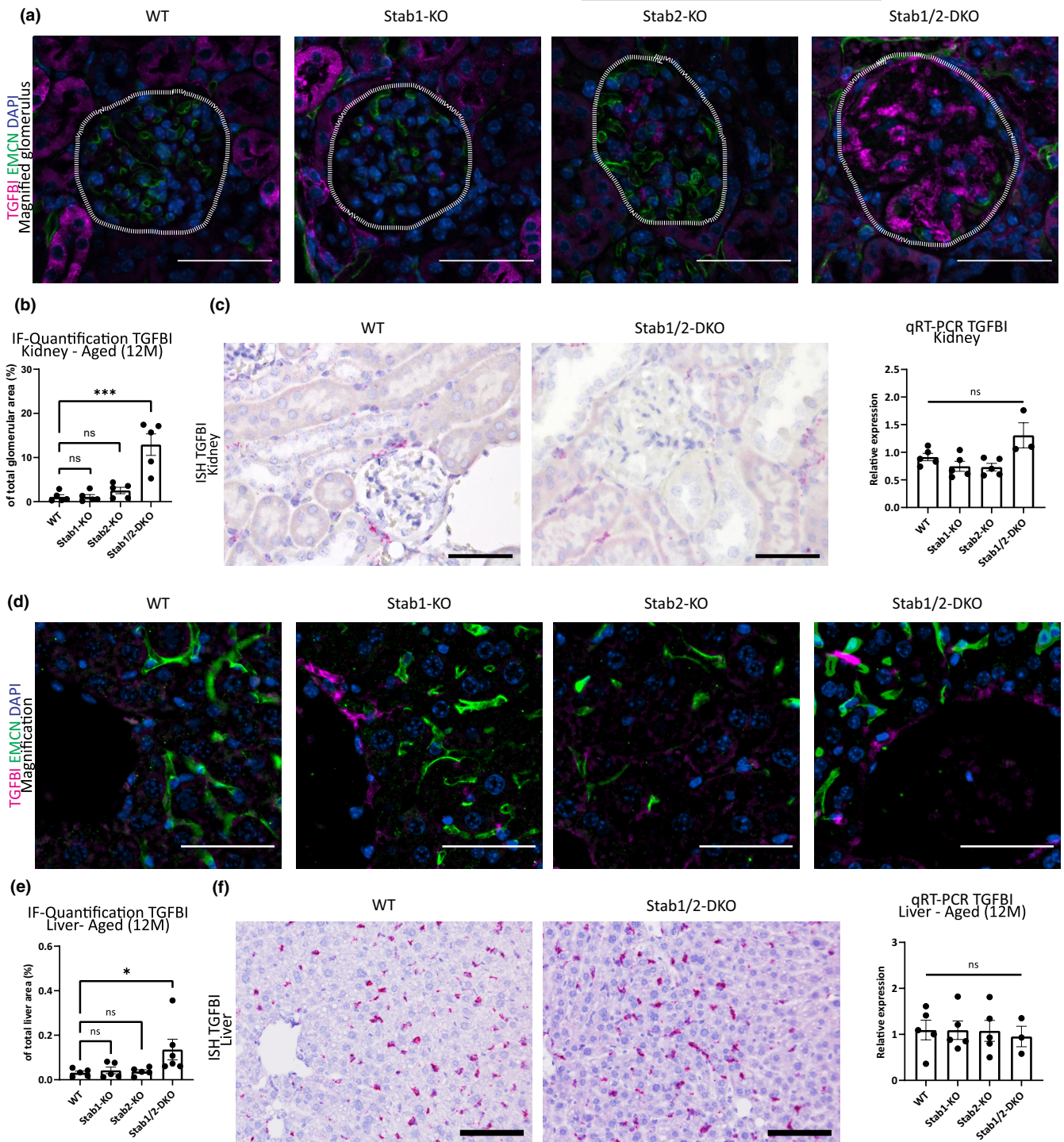
FIGURE 4 Abundance of TGFBI in organs from Stabilin-deficient animals. (a) Representative photomicrographs of kidney tissue (upper lane: Overview; lower lane: Magnified glomeruli, Scale bar = 50 μm) co-stained with DAPI (blue), Emcn (green), and TGFBI (magenta). Dashed white line marks glomeruli (b) Quantification of average TGFBI-positive area in glomeruli (in % of total glomerular area, $n \geq 5$). (c) Left panel: In situ hybridization (Scale bar = 50 μm) and right graph: rt-PCR of kidney tissue in WT and Stab-DKO animals for TGFBI ($n \geq 3$). (d) Representative photomicrographs of liver tissue (upper lane: Overview; lower lane: Magnified pericentral area, Scale bar = 50 μm) co-stained with DAPI (blue), Emcn (green), and TGFBI (magenta). (e) Quantification of average TGFBI-positive area of total photomicrograph area (in % of total photomicrograph area, $n \geq 5$). (f) Left panel: In situ hybridization (Scale bar = 100 μm) and Right graph: rt-PCR ($n \geq 3$) of kidney tissue in WT and Stab-DKO animals for TGFBI. ns = not significant, $*p < 0.05$; $**p < 0.01$; $***p < 0.001$.

Quantification of TGFBI intensity in aged glomeruli revealed significantly more TGFBI in Stab-DKO glomeruli compared to WT, while Stab1-KO and Stab2-KO glomeruli did not exhibit significantly more

TGFBI (Figure 4b). Similarly to POSTN, we performed RNA-ISH for TGFBI in glomeruli of aged Stab-DKO mice in comparison to WT mice as well as qRT-PCR of kidney lysate which did not show any

differences, pointing toward a deposition of TGFBI from the plasma (Figure 4c).

Since POSTN was found to be more abundant in Stab-DKO livers, we also analyzed liver tissue for TGFBI abundance. Here, similarly to the kidney, we found a pronounced increase in TGFBI levels only in Stab-DKO livers compared to WT in immunofluorescence (Figure 4d,e) and no increased transcription using RNA-ISH and qRT-PCR (Figure 4f).

To confirm antibody specificity, we performed Simple-Western (Figure S4a) and Western Blotting (Figure S4b), which revealed increased TGFBI abundance in kidney and liver lysate of Stab-DKO animals. No overt changes were observed in Stab1-KO und Stab2-KO liver and kidney tissue in comparison to WT mice, although a small but significant increase was found in Stab2-KO livers using simple Western, which could not be confirmed with other methods.

3.5 | TGFBI depositions occur independently of POSTN in Stab-DKO tissue

Previously, we have demonstrated that POSTN and TGFBI are both ligands of Stab1 and Stab2, likely due to their structure and binding of fasciclin domains. Since TGFBI and POSTN revealed similar staining patterns in Stab-DKO animals, we correlated TGFBI and POSTN abundance in single glomeruli and found a strong and significant correlation in Stab-DKO, but not WT glomeruli (Figure 5a). As TGFBI and POSTN may directly interact via their Fasciclin domains, we checked whether increased TGFBI abundance in glomeruli and liver tissue occurs independently of POSTN in Stabilin-DKO mice. Comparison of TGFBI abundance in WT, Stab-DKO, and Stab-POSTN-TrKO kidney and liver tissue revealed increased TGFBI abundance in Stab-DKO and Stab-POSTN-TrKO compared to wildtype control mice, indicating independence of TGFBI abundance in kidney (Figure 5b) and liver tissue (Figure 5c) in Stab-DKO mice from POSTN. We saw a midzonal (sinusoidal distribution of TGFBI in the liver lobulus in all genotypes as indicated by pericentral LSEC marker EMCN (Figure 5c).

3.6 | POSTN and TGFBI positivity in liver and kidney is detected in early adult age in Stab-DKO and increases during aging

Since we could show strong positivity of TGFBI and POSTN in aged Stab-DKO mice which already show a pronounced proteinuria, we investigated whether 3-month-old animals show similar staining patterns in the kidney and liver. Here, we observed a strong increase of POSTN (Figure 6a) and TGFBI (Figure 6b) positive area in glomeruli of young Stab-DKO mice compared to young WT controls. A slight increase in TGFBI-positive glomerular area was observed in Stab2-KO glomeruli compared to WT. Comparing glomeruli from young mice to aged mice revealed that ligand abundance did not change in WT and Stab2-KO mice, while Stab1-KO mice showed significantly more POSTN positive area in aged glomeruli and Stab-DKO mice showed

an age-dependent increase for TGFBI and a likely trend for POSTN ($p = 0.1457$).

4 | DISCUSSION

We here show that scavenging by Stab1 and Stab2 is crucial not only for homeostasis of TGFBI and POSTN plasma levels in mice (Manta et al., 2022), but also to prevent age-dependent accumulation of TGFBI and POSTN in liver and kidney tissue. We hypothesize that POSTN and TGFBI are not produced locally in Stab-DKO livers and kidneys, but are deposited in these organs, possibly due to their high concentrations in Stab-DKO plasma, since their scavenger receptors are missing. This hypothesis is supported by constant mRNA levels in the liver and kidney as shown here by RNA-ISH and qRT-PCR (Figures 2 and 4f). As we have shown previously, transcriptomic data from isolated LSECs show a slight but significant downregulation of POSTN in LSECs from Stabilin deficient animals compared to WT animals (Olsavszky et al., 2021). POSTN and TGFBI staining co-localized in liver and glomeruli and was largely confined to the midzonal, perisinusoidal area in the liver, with a similar pattern compared to Sirius-red positive areas (Figure 5c, Figure S3). We here observed partial co-localization with Collagen 1 staining in glomeruli and liver tissue, indicating a similar, but not identical pattern (Figure S3).

In mice and humans, there are somewhat contradictory findings regarding age-dependent plasma levels of TGFBI and POSTN. In mice, it was described that TGFBI and POSTN plasma levels are decreased in aged mice (Yang et al., 2020), while human data show an increase in aged populations (Lehallier et al., 2019). Since aging in mice and humans differ considerably, we can only speculate on the biological relevance of decreased TGFBI and POSTN plasma abundance in aged WT mice. Since we were able to find increased deposition of both Stabilin ligands in glomeruli of aged knockout mice compared to younger mice, we could further underline the hypothesis of a time-dependent deposition from plasma in our models.

Interestingly, ablation of POSTN in Stab-DKO mice did not rescue the reduced lifespan (Figure 3a, Figure S1). Furthermore, knock-out of POSTN did not affect levels of TGFBI in glomeruli and livers of Stab-DKO mice (Figure 5b,c), indicating that TGFBI depositions occur independently of POSTN. In comparison to Stab-DKO, a reduced average glomerular diameter and increased vascularization in Stab-POSTN-TrKO were observed, which did not influence survival or protein levels in urine (Figure 3). In summary, these findings point toward a slight amelioration of the kidney phenotype by deletion of POSTN in Stab-DKO. Since knockout of POSTN alone has been shown to ameliorate deterioration of kidney fibrosis (An et al., 2021), reduction of POSTN-dependent fibrosis in Stab-POSTN-TrKO mice is a likely explanation for this observation. Unchanged survival in Stab-POSTN-TrKO indicates that other alterations of ligands are responsible for the reduced life span. It was previously reported that amelioration of liver fibrosis occurs in pro-fibrotic models in POSTN-deficient mice (Huang et al., 2015; Kumar et al., 2018). As we did not observe alterations of liver fibrosis in Stab-POSTN-TrKO mice
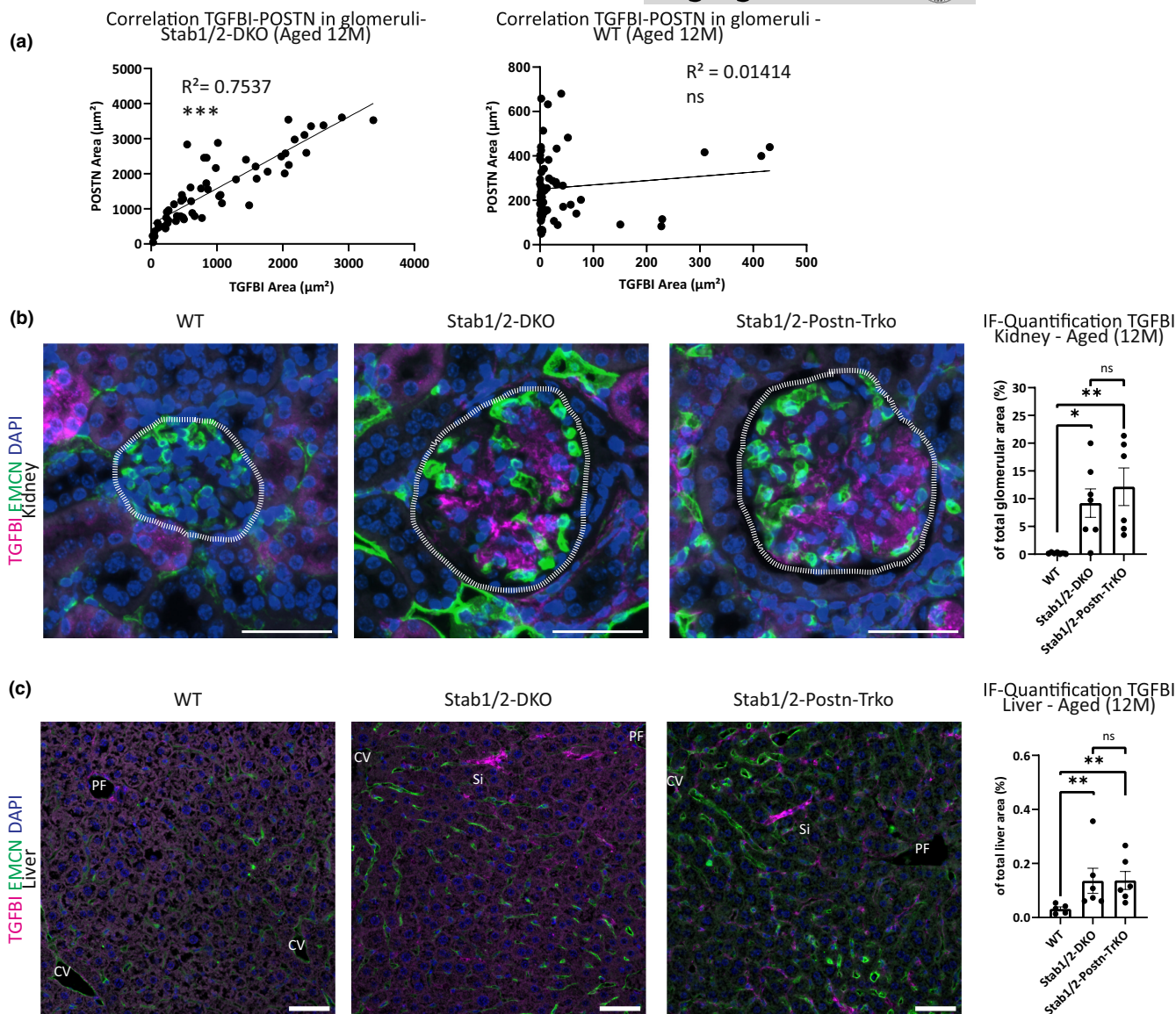
FIGURE 5 Stab-TrKO mice share similar TGFBI depositions in liver and kidney with Stab-DKO mice. (a)Correlation of TGFBI and POSTN abundance from quantified immunofluorescent microphotographs in kidney tissue of DKO (left panels) and WT (right panels) mice. (b) Representative photomicrographs of kidney tissue co-stained with DAPI (blue), Emcn (green), and TGFBI (magenta). Dashed white line marks glomeruli. Right panel: Quantification of average TGFBI-positive area in glomeruli (in % of total glomerular area). (c) Representative photomicrographs of liver tissue co-stained with DAPI (blue), Emcn (green), and TGFBI (magenta). Right panel: Quantification of average TGFBI-positive area of total photomicrograph area (in % of total photomicrograph area). $N \geq 5$ for all experiments. Scale bar$=50\,\mu m$. Ns$=$not significant, $*p<0.05$; $**p<0.01$; $***p<0.001$.

compared to Stab1/2-DKO mice (Figure S2b), this indicates alternative mechanisms of liver fibrosis that are independent of POSTN in Stab1/2-DKO mice.

Whether TGFBI is solely responsible for the possibly fatal glomerulofibrosis in Stab-DKO and Stab-POSTN-TrKO is unclear, since we observed more than 100 dysregulated proteins comparing the plasma proteome of Stab-DKO mice compared to WT mice (Manta et al., 2022). Stab1 and Stab2 not only contain fasciclin domains, but also EGF-like domains and Laminin EGF-like domains beside the X-link domain (Politz et al., 2002). The EGF-like domain containing protein Reelin has previously been identified by us as a Stabilin-2 ligand (Manta et al., 2022). No Reelin depositions were found in kidneys

and livers of our models (data not shown). Other proteins elevated in the plasma of Stabilin deficient mice containing EGF-like domains and Laminin EGF-like domains are putative ligands of Stabilin receptors and will be scrutinized in further experiments.

These findings bear consequences for the use of therapeutical inhibition of Stabilins, which for Stab1 is already in Phase 2 clinical trials in cancer (Virtakoivu et al., 2021) and might be a treatment option for atherosclerosis in future studies (Manta et al., 2022). Single deficiency for Stab1 or Stab2 alone did not seem to induce strong damage to kidney function, although a mild increase in TGFBI depositions was observed in young, but not aged Stab2-KO glomeruli. It can be assumed that absence of one of the

LEIBING ET AL.
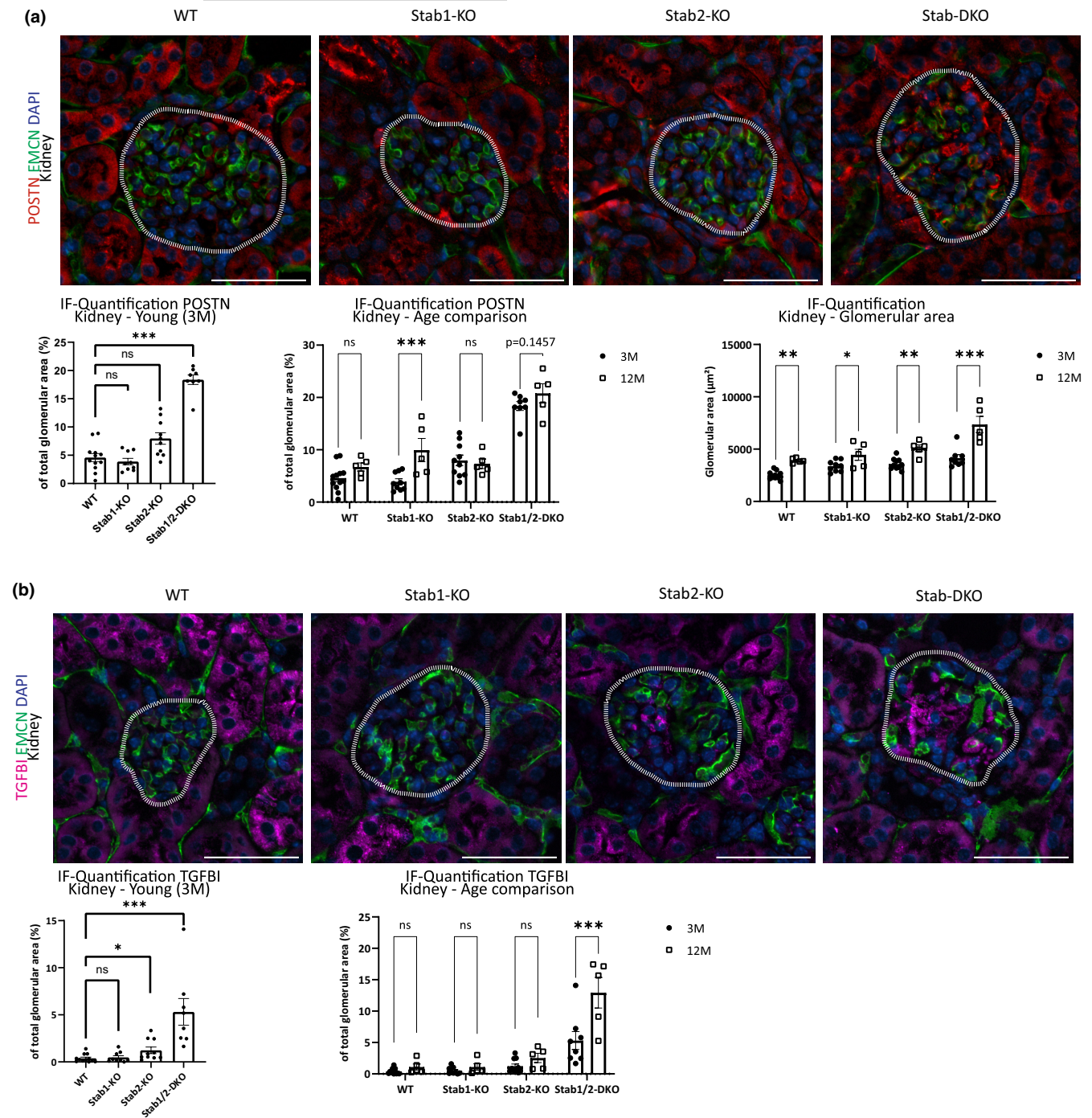
FIGURE 6 Age-dependent ligand abundance in glomeruli. (a) Representative photomicrographs of kidney tissue co-stained with DAPI (blue), Emcn (green), and POSTN (red). Dashed white line marks glomeruli. Lower left panel: Quantification of average POSTN-positive area in glomeruli (in % of total glomerular area). Lower middle panel: Glomerular POSTN-positive area in glomeruli (in % of total glomerular area) in 3- and 12-months old mice. Lower right panel: Glomerular area in μm^2 in different age groups and genotypes. (b) Representative photomicrographs of kidney tissue co-stained with DAPI (blue), Emcn (green), and TGFBI (magenta). Dashed white line marks glomeruli. Lower left panel: Quantification of average TGFBI-positive area in glomeruli (in % of total glomerular area). Lower right panel: Glomerular TGFBI-positive area in glomeruli (in % of total glomerular area) in 3- and 12-months old mice. $n \geq 5$ for all experiments. Scale bar $= 50\,\mu m$. ns $=$ not significant, $^*p < 0.05$; $^{**}p < 0.01$; $^{***}p < 0.001$.

Stabilins can be compensated for by the respective other Stabilin and only double-knockout is detrimental, which is in line with previous findings from our group (Manta et al., 2022; Schledzewski et al., 2011). In summary, we do not expect grave side effects form

antibody-mediated Stabilin-inhibition, which is usually transient and not as strong as genetic deficiency for one or even both Stab1 and Stab2. Previous transcriptomic analysis of LSECs revealed the most drastic changes in Stab-DKO compared to WT, Stab1-KO

and Stab2-KO as well (Olsavszky et al., 2021). Nevertheless, side effects of anti-Stabilin targeted therapies in individuals with decreased renal or liver function cannot be ruled out and should be monitored closely.

To conclude, we were able to further validate our previous findings that the four fasciclin proteins Stab1, Stab2, POSTN, and TGFBI constitute a ligand-scavenger receptor system without any relevant compensation by other scavenger receptors. While targeted inhibition of Stab1 or Stab2 might be beneficial in the context of atherosclerosis prevention, double deficiency leads to premature organ failure likely due to multi-ligand depositions caused by deficient hepatic scavenging.

DATA AVAILABILITY STATEMENT

The data that support the findings of this study are available from the corresponding author upon reasonable request.

ORCID

Thomas Leibing https://orcid.org/0000-0002-7157-1201

REFERENCES

An, J. N., Kim, H., Kim, E. N., Cho, A., Cho, Y., Choi, Y. W., Kim, J. H., Yang, S. H., Choi, B. S., Lim, C. S., Kim, Y. S., Kim, K. P., & Lee, J. P. (2021). Effects of periostin deficiency on kidney aging and lipid metabolism. *Aging (Albany NY)*, *13*(19), 22649–22665. https://doi.org/10.18632/aging.203580

An, J. N., Yang, S. H., Kim, Y. C., Hwang, J. H., Park, J. Y., Kim, D. K., Kim, J. H., Kim, D. W., Hur, D. G., Oh, Y. K., Lim, C. S., Kim, Y. S., & Lee, J. P. (2019). Periostin induces kidney fibrosis after acute kidney injury via the p38 MAPK pathway. *American Journal of Physiology. Renal Physiology*, *316*(3), F426–f437. https://doi.org/10.1152/ajprenal.00203.2018

Bhandari, S., Larsen, A. K., McCourt, P., Smedsrød, B., & Sørensen, K. K. (2021). The scavenger function of liver sinusoidal endothelial cells in health and disease. *Frontiers in Physiology*, *12*. https://doi.org/10.3389/fphys.2021.757469

Billings, P. C., Whitbeck, J. C., Adams, C. S., Abrams, W. R., Cohen, A. J., Engelsberg, B. N., Howard, P. S., & Rosenbloom, J. (2002). The transforming growth factor-β-inducible matrix protein βig-h3 interacts with fibronectin. *Journal of Biological Chemistry*, *277*(31), 28003–28009. https://doi.org/10.1074/jbc.M106837200

Guerrot, D., Dussaule, J. C., Mael-Ainin, M., Xu-Dubois, Y. C., Rondeau, E., Chatziantoniou, C., & Placier, S. (2012). Identification of periostin as a critical marker of progression/reversal of hypertensive nephropathy. *PLoS One*, *7*(3), e31974. https://doi.org/10.1371/journal.pone.0031974

Hansen, B., Longati, P., Elvevold, K., Nedredal, G. I., Schledzewski, K., Olsen, R., Falkowski, M., Kzhyshkowska, J., Carlsson, F., Johansson, S., Smedsrød, B., Goerdt, S., Johansson, S., & McCourt, P. (2005). Stabilin-1 and stabilin-2 are both directed into the early endocytic pathway in hepatic sinusoidal endothelium via interactions with clathrin/AP-2, independent of ligand binding. *Experimental Cell Research*, *303*(1), 160–173. https://doi.org/10.1016/j.yexcr.2004.09.017

Hanssen, E., Reinboth, B., & Gibson, M. A. (2003). Covalent and non-covalent interactions of βig-h3 with collagen VI: βig-h3 IS COVALENTLY ATTACHED TO THE AMINO-TERMINAL REGION OF COLLAGEN VI IN TISSUE MICROFIBRILS*. *Journal of Biological Chemistry*, *278*(27), 24334–24341. https://doi.org/10.1074/jbc.M303455200

Harris, E. N., & Cabral, F. (2019). Ligand binding and signaling of HARE/Stabilin-2. *Biomolecules*, *9*(7), 273. https://doi.org/10.3390/biom9070273

Harris, V. M. (2015). Protein detection by simple Western™ analysis. *Methods in Molecular Biology*, *1312*, 465–468. https://doi.org/10.1007/978-1-4939-2694-7_47

Huang, Y., Liu, W., Xiao, H., Maitikabili, A., Lin, Q., Wu, T., Huang, Z., Liu, F., Luo, Q., & Ouyang, G. (2015). Matricellular protein periostin contributes to hepatic inflammation and fibrosis. *The American Journal of Pathology*, *185*(3), 786–797. https://doi.org/10.1016/j.ajpath.2014.11.002

Kumar, P., Smith, T., Raeman, R., Chopyk, D. M., Brink, H., Liu, Y., Sulchek, T., & Anania, F. A. (2018). Periostin promotes liver fibrogenesis by activating lysyl oxidase in hepatic stellate cells. *The Journal of Biological Chemistry*, *293*(33), 12781–12792. https://doi.org/10.1074/jbc.RA117.001601

Lehallier, B., Gate, D., Schaum, N., Nanasi, T., Lee, S. E., Yousef, H., Moran Losada, P., Berdnik, D., Keller, A., Verghese, J., Sathyan, S., Franceschi, C., Milman, S., Barzilai, N., & Wyss-Coray, T. (2019). Undulating changes in human plasma proteome profiles across the lifespan. *Nature Medicine*, *25*(12), 1843–1850. https://doi.org/10.1038/s41591-019-0673-2

Leibing, T., Geraud, C., Augustin, I., Boutros, M., Augustin, H. G., Okun, J. G., Okun, J. G., Langhans, C. D., Zierow, J., Wohlfeil, S. A., Olsavszky, V., Schledzewski, K., Goerdt, S., & Koch, P. S. (2018). Angiocrine Wnt signaling controls liver growth and metabolic maturation in mice. *Hepatology*, *68*(2), 707–722. https://doi.org/10.1002/hep.29613

Lück, C., Haitjema, C., & Heger, C. (2021). Simple Western: Bringing the Western blot into the twenty-first

century. *Methods in Molecular Biology*, *2261*, 481–488. https://doi.org/10.1007/978-1-0716-1186-9_30

Manta, C.-P., Leibing, T., Friedrich, M., Nolte, H., Adrian, M., Schledzewski, K., Krzistetzko, J., Kirkamm, C., David Schmid, C., Xi, Y., Stojanovic, A., Tonack, S., de la Torre, C., Hammad, S., Offermanns, S., Krüger, M., Cerwenka, A., Platten, M., Goerdt, S., & Géraud, C. (2022). Targeting of scavenger receptors Stabilin-1 and Stabilin-2 ameliorates atherosclerosis by a plasma proteome switch mediating monocyte/macrophage suppression. *Circulation*, *146*(23), 1783–1799. https://doi.org/10.1161/CIRCULATIONAHA.121.058615

Oka, T., Xu, J., Kaiser, R. A., Melendez, J., Hambleton, M., Sargent, M. A., Lorts, A., Brunskill, E. W., Dorn, G. W., 2nd, Conway, S. J., Aronow, B. J., Robbins, J., & Molkentin, J. D. (2007). Genetic manipulation of periostin expression reveals a role in cardiac hypertrophy and ventricular remodeling. *Circulation Research*, *101*(3), 313–321. https://doi.org/10.1161/circresaha.107.149047

Olsavszky, V., Sticht, C., Schmid, C. D., Winkler, M., Wohlfeil, S. A., Olsavszky, A., Schledzewski, K., Géraud, C., Goerdt, S., Leibing, T., & Koch, P. S. (2021). Exploring the transcriptomic network of multi-ligand scavenger receptor Stabilin-1- and Stabilin-2-deficient liver sinusoidal endothelial cells. *Gene*, *768*, 145284. https://doi.org/10.1016/j.gene.2020.145284

Patten, D. A., & Shetty, S. (2019). The role of Stabilin-1 in lymphocyte trafficking and macrophage scavenging in the liver microenvironment. *Biomolecules*, *9*(7), 283. https://doi.org/10.3390/biom9070283

Politz, O., Gratchev, A., McCourt, P. A., Schledzewski, K., Guillot, P., Johansson, S., Svineng, G., Franke, P., Kannicht, C., Kzhyshkowska, J., Longati, P., Velten, F. W., Johansson, S., & Goerdt, S. (2002). Stabilin-1 and-2 constitute a novel family of fasciclin-like hyaluronan receptor homologues. *The Biochemical Journal*, *362*(Pt 1), 155–164. https://doi.org/10.1042/0264-6021:3620155

PrabhuDas, M. R., Baldwin, C. L., Bollyky, P. L., Bowdish, D. M. E., Drickamer, K., Febbraio, M., Herz, J., Kobzik, L., Krieger, M., Loike, J., McVicker, B., Means, T. K., Moestrup, S. K., Post, S. R., Sawamura, T., Silverstein, S., Speth, R. C., Telfer, J. C., Thiele, G. M., ... El Khoury, J. (2017). A consensus definitive classification of scavenger receptors and their roles in health and disease. *Journal of Immunology*, *198*(10), 3775–3789. https://doi.org/10.4049/jimmunol.1700373

Satirapoj, B., Tassanasorn, S., Charoenpitakchai, M., & Supasyndh, O. (2015). Periostin as a tissue and urinary biomarker of renal injury in type 2 diabetes mellitus. *PLoS One*, *10*(4), e0124055. https://doi.org/10.1371/journal.pone.0124055

Satirapoj, B., Witoon, R., Ruangkanchanasetr, P., Wantanasiri, P., Charoenpitakchai, M., & Choovichian, P. (2014). Urine periostin as a biomarker of renal injury in chronic allograft nephropathy. *Transplantation Proceedings*, *46*(1), 135–140. https://doi.org/10.1016/j.transproceed.2013.07.069

Schledzewski, K., Geraud, C., Arnold, B., Wang, S., Grone, H. J., Kempf, T., Wollert, K. C., Straub, B. K., Schirmacher, P., Demory, A., Schönhaber, H., Gratchev, A., Dietz, L., Thierse, H. J., Kzhyshkowska, J., & Goerdt, S. (2011). Deficiency of liver sinusoidal scavenger receptors stabilin-1 and-2 in mice causes glomerulofibrotic nephropathy via impaired hepatic clearance of noxious blood factors. *The Journal of Clinical Investigation*, *121*(2), 703–714. https://doi.org/10.1172/jci44740

Schneider, C. A., Rasband, W. S., & Eliceiri, K. W. (2012). NIH image to ImageJ: 25 years of image analysis. *Nature Methods*, *9*(7), 671–675. https://doi.org/10.1038/nmeth.2089

Schwanekamp, J. A., Lorts, A., Vagnozzi, R. J., Vanhoutte, D., & Molkentin, J. D. (2016). Deletion of Periostin protects against atherosclerosis in mice by altering inflammation and extracellular matrix remodeling. *Arteriosclerosis, Thrombosis, and Vascular Biology*, *36*(1), 60–68. https://doi.org/10.1161/ATVBAHA.115.306397

Seifert, G. J. (2018). Fascinating Fasciclins: A surprisingly widespread family of proteins that mediate interactions between the cell exterior and the cell surface. *International Journal of Molecular Sciences*, *19*(6), 1628. https://doi.org/10.3390/ijms19061628

Virtakoivu, R., Rannikko, J. H., Viitala, M., Vaura, F., Takeda, A., Lönnberg, T., Koivunen, J., Jaakkola, P., Pasanen, A., Shetty, S., de Jonge, M. J. A., Robbrecht, D., Ma, Y. T., Skyttä, T., Minchom, A., Jalkanen, S., Karvonen, M. K., Mandelin, J., Bono, P., & Hollmén, M. (2021). Systemic blockade of Clever-1 elicits lymphocyte activation alongside checkpoint molecule downregulation in patients with solid tumors: Results from a phase I/II clinical trial. *Clinical Cancer Research*, *27*(15), 4205–4220. https://doi.org/10.1158/1078-0432.Ccr-20-4862

Wantanasiri, P., Satirapoj, B., Charoenpitakchai, M., & Aramwit, P. (2015). Periostin: A novel tissue biomarker correlates with chronicity index and renal function in lupus nephritis patients. *Lupus*, *24*(8), 835–845. https://doi.org/10.1177/0961203314566634

Yang, Y. R., Kabir, M. H., Park, J. H., Park, J. I., Kang, J. S., Ju, S., Shin, Y. J., Lee, S. M., Lee, J., Kim, S., Lee, K. P., Lee, S. Y., Lee, C., & Kwon, K. S. (2020). Plasma proteomic profiling of young and old mice reveals cadherin-13 prevents age-related bone loss. *Aging (Albany NY)*, *12*(9), 8652–8668. https://doi.org/10.18632/aging.103184

SUPPORTING INFORMATION

Additional supporting information can be found online in the Supporting Information section at the end of this article.